PNAS
www.pnas.org

Supplementary Information for:

Targeting presynaptic H3 heteroreceptor in nucleus accumbens to improve anxiety and obsessive-compulsive-like behaviors

Xiao-Yang Zhang, Shi-Yu Peng, Li-Ping Shen, Qian-Xing Zhuang, Bin Li, Shu-Tao Xie, Qian-Xiao Li, Ming-Run Shi, Tian-Yu Ma, Qi-Peng Zhang, Jian-Jun Wang, Jing-Ning Zhu

Corresponding authors: Jing-Ning Zhu; Bin Li

Emails: jnzhu@nju.edu.cn (J.-N.Z.) or bli@nju.edu.cn (B.L.)

This PDF file includes:

www.pnas.org/cgi/doi/10.1073/pnas.2008456117

Supplementary Materials and Methods

Animals. HDC-Cre and wild-type Sprague-Dawley (SD) rats were individually housed on a 12 h light/dark cycle with water available *ad libitum*. All experiments, approved by the Animal Ethical and Welfare Committee of Nanjing University, were conducted in accordance with U.S. National Institutes of Health Guide for the Care and Use of Laboratory Animals (1). All efforts were made to minimize the number of animals used and their suffering.

Generation of HDC-Cre rats. The HDC-Cre rats were generated using CRISPR/Cas9 technology. Briefly, a P2A-Cre cassette was targeted into the coding sequence of exon 12 and 3′UTR of the HDC gene. The Cas9/sgRNA and targeting vectors were injected into the cytoplasm of one-cell stage embryos through the injection needle. Injected zygotes were transferred into pseudopregnant female SD rats after 2 h culture in KSOM medium to generate the strain, which was maintained on a SD genetic background (Beijing Biocytogen Co., Ltd., China). The F0 chimera rats were crossed with wild-type rats to get the germline transmission F1 rats. The correct targeting of the P2A-Cre in F1 rats was confirmed by gene sequencing (*SI Appendix*, Fig. S3A-C) and Southern blot (*SI Appendix*, Fig. S3D-E). The primers for genotyping are as follows: WT-forward: 5’-GGT CTC TGT GTG GGT GAT GTG ACA G-3’ and Mut-reverse: 5’-TCT TGG TCC TGC CAA TGT GGA TCA G-3’; Mut-forward: 5’-GGA AAT GGT TCC CTG CTG AAC CTG A-3’ and WT-reverse: 5’-ATC TAA GGG CCT CAA AGT GCA GAC C-3′. For further validation of the transgene’s expression, the HDC-Cre rats were crossed with Rosa26-LSL-tdTomato

reporter rats (SD-Gt(ROSA)26Sortm1(CAG-LSL-tdTomato)/Bcgen; stock#B-CR-011; Beijing Biocytogen Co., Ltd).

Anterograde tracing. The experimental procedures for anterograde tracing followed our previous report (2-4). After anesthesia by intraperitoneal injection of sodium pentobarbital (40 mg/kg), the rats of either sex were placed into a stereotaxic frame (1404, David Kopf Instrument, Tujunga, CA) for brain surgery. A 1 to 2 cm incision was made in the scalp, and a small hole was drilled in the skull. A glass micropipette (WPI, Sarasota, FL) with the inner tip diameter of 10 to 15 μm was filled with 10% biotinylated dextran amine (BDA; Molecular Probes, Leiden, The Netherlands, Cat# D1956) in 0.01 M phosphate buffered saline (PBS; pH 7.4) and lowered slowly into the tuberomammillary nucleus (TMN) of the hypothalamus at the coordinates of Bregma anteroposterior -4.5 mm, mediolateral 1.2 mm, and dorsoventral 9.6 mm according to the rat brain atlas of Paxinos and Watson (5). Iontophoresis were made under 5 μA positive alternating current (7s on/7s off) for 40 min. Once completed, the micropipette was left in place for 10 min before removal. During micropipette withdrawal, the current was reversed to minimize tracer leakage through the injection tract. Rats that received successful tracer injections were allowed to survive for three weeks before the terminal experiment was conducted.

Immunohistochemistry. Immunostainings were conducted as our previous reports (2, 4, 6, 7). Rats of either sex were anesthetized with sodium pentobarbital and perfused transcardially with 100 ml normal saline, followed by 250 to 300 ml 4 % paraformaldehyde or 4% *N*-(3-Dimethylaminopropyl)-*N'*-ehylcarbodiimide hydrochloride (EDAC; Sigma-

Aldrich, St. Louis, MO; for histamine immunostaining experiment) in 0.1 M phosphate buffer. Subsequently, the brain was removed, trimmed and postfixed in 4% paraformaldehyde overnight, or 4% EDAC for 4 h followed by 4% paraformaldehyde overnight (for histamine immunostaining), at 4 °C. Then the brain was cryoprotected with 20% sucrose and then 30% sucrose for 24 h. Frozen coronal sections (25 μm thick) containing the TMN, NAc core, PrL, BLA or vHipp were obtained by using a freezing microtome (CM3050S, Leica, Germany) and mounted on gelatin-coated slides. The slices were rinsed with PBS containing 0.1% Triton X-100 (PBST) and then incubated in 10% normal bovine serum in PBST for 30 min.

Sections were incubated overnight at 4 °C with primary antibodies against histamine (a rabbit anti-histamine antibody, 1:500; Acris, Herford, Germany, Cat# 22939), GAD67 (a mouse anti-GAD67 monoclonal antibody, 1:1000; Sigma, Cat# G5419), H3 receptor (a rabbit anti-histamine H3 antibody, 1:500; Acris, Cat# SP4355P), VGLUT1 (a guinea pig anti-VGLUT1 antibody, 1:500; Millipore, Billerica, MA, Cat# AB5905), VGLUT2 (a mouse anti-VGLUT2 antibody, 1:500; Abcam, Cambridge, MA, Cat# AB79157), and glutamate (a mouse anti-Glutamate antibody, 1:500; Millipore, Billerica, MA, Cat# AB94698). After a complete wash in PBS, the sections were incubated in the related secondary antibodies (1:2000; Invitrogen) conjugated to AlexaFluor 488, AlexaFluor 594, and AlexaFluor 405 for 2 h at room temperature in the dark. The slides were washed and mounted in Fluoromount-G mounting medium (Southern Biotech, Birmingham, AL). Incubations replacing the primary antiserum with control immunoglobulins and/or omitting the primary antiserum were used as negative controls. All micrographs were taken

with an inverted laser scanning confocal FluoView FV1000 microscope (Olympus, Tokyo, Japan). Digital images from the microscope were recorded with FV10-ASW 3.1 Viewer Software (Olympus) and image processing was done with Photoshop (Adobe systems Inc, San Jose, CA).

Western blot. Rat brain homogenates of either sex in buffer (50 mM Tris-HCl, pH 7.4, 150 mM NaCl, 50 mM NaF, 1.0 mM Na_3VO_4, 2.0 mM EDTA, 5 mM 4-(2-aminoethyl) benzenesulfonyl fluoride hydrochloride (AEBSF), 10 μg/mL leupeptin, 10 μg/mL aprotinin, and 10 μg/mL pepstatin) were diluted in 2 × Laemmli SDS sample buffer at 1:1 ratio, followed by heating at 95 °C for 5 min. The protein concentration was determined by using A660 kit (Pierce Rockford, IL) according to manufactory manual. Proteins were firstly resolved in SDS-PAGE, and the proteins in the gels were transferred onto Immobilon-P membrane (Millipore, Billerica, MA), followed by incubation with primary antibody, anti-histamine H3 receptor (1:250, Santa Cruz, Dallas, TX, Cat# sc-50311)/actin (1:5000, Sigma, Cat# A1978) washing and incubation with HRP-conjugated goat anti-rabbit IgG (H+L) secondary antibody (Thermo Scientific, Waltham, MA, Cat# 31460). The protein-antibody complexes were visualized by the Pierce ECL Western Blotting Substrate (Thermo Scientific) and exposed to Kodak medical X-ray film (Denville Scientific Inc, Holliston, MA).

Stereotaxic implantation and microinjection. Male rats weighing 230 to 250 g were used in the behavioral tests. The rats were anesthetized with sodium pentobarbital in a dose of 40 mg/kg intraperitoneally and then mounted on a stereotaxic frame (1404, David Kopf

Instruments) for brain surgery under aseptic conditions. Two stainless-steel guide tubes (length 11 mm, outer diameter 0.8 mm, inner diameter 0.5 mm) for the microinjection cannulae were bilaterally implanted into the cerebrum of each animal. The lower ends of guide tubes were positioned 2.0 mm above the NAc core (anteroposterior 1.3 mm, mediolateral 1.5 mm, and dorsoventral 6.5 mm). Rats were caged individually and allowed to recover for at least 72 h.

During the behavioral testing sessions, two stainless-steel injection cannulae (length 13 mm, outer diameter 0.5 mm, inner diameter 0.3 mm) were inserted to protrude 2 mm beyond the tip of the guide tube and just above the NAc core (to minimize lesioning the nuclei) for microinjection of histamine (0.5 μg; Sigma-Aldrich), RAMH (a selective H3 receptor agonist, 0.5 μg; Tocris Bioscience, Bristol, UK), iodophenpropit (IPP, a selective H3 receptor antagonist, 1.5 μg; Tocris Bioscience), and saline (0.9% NaCl) using Hamilton syringes (0.5 μl each side, lasting 2 min). The effective extent of the drug diffusion in the present study was restricted in the NAc core according to the estimate by extracellular electrophysiological recording units 0.5 to 2.0 mm away from the injection site as our previous report (3). Data from rats in which the injection sites were histologically identified to be deviated from the NAc core were excluded from further analysis.

Optogenetic manipulation. For virus injections, 0.5 μL of AAV2/9-hEF1α-DIO-ChR2-mCherry/AAV2/9-hEF1α-DIO-mCherry (Taitool, Shanghai, China) or pAAV-CaMKIIα-ChR2-mCherry/pAAV-CaMKIIα-mCherry (Obio, Shanghai, China) was bilaterally infused to hypothalamic TMN (anteroposterior -4.5 mm, mediolateral 1.2 mm, and

dorsoventral 9.6 mm) and PrL (anteroposterior +3.0 mm, mediolateral 0.7 mm, and dorsoventral 3.3 mm), BLA (anteroposterior -2.1 mm, mediolateral 5.0 mm, dorsoventral 8.6 mm) or vHipp (anteroposterior -6.0 mm, mediolateral 5.0 mm, dorsoventral 8.0 mm) through 33 gauge needles (0.07 µL/min for 7 min). Following viral injection, needles were kept at the injection site for 10 min to allow for viral diffusion. For TMN-, PrL-, BLA- and vHipp-NAc core terminal photo-stimulation, rats received chronically implantable optical fibers (200 µm core; 0.37 numerical aperture; Newdoon; Hangzhou, China) aimed over the NAc core. Three to four weeks were allowed for viral expression before behavioral testing.

To permit bilateral manipulation, the single end of 2 × 1 fiber splitter (Newdoon) was connected to a rotating commutator (Doric, Quebec, Canada), which was then attached via a fiber to a laser (Newdoon). Light output was measured with an optical power meter and adjusted to 7 mW of 473 nm light. For photostimulation of the TMN-NAc core histaminergic afferent terminals before the exposure to acute restraint stress, blue light was applied at 10 ms pulse width and a frequency of 10 Hz for 8 min (8). For photostimulation of the PrL-, BLA- and vHipp-NAc core glutamatergic afferent terminals during the anxiety- and obsessive-compulsive-like behavioral tests, blue light with 5 ms pulse width and a frequency of 20 Hz, 20 Hz and 4 Hz, respectively, was delivered (9, 10).

Chemogenetic manipulation. For chemogenetic inhibition of PrL- and BLA-NAc core projections, a retrograde traveling Cre-recombinase (AAV2/2 Retro Plus-hSyn-Cre-EGFP, 0.5 µL, Taitool, Shanghai, China) was bilaterally infused into NAc core (anteroposterior 1.3, mediolateral 1.5, and dorsoventral 6.5), while AAV vectors expressing Cre-dependent

hM4Di (AAV2/9-hSyn-DIO-hM4Di)-mCherry, 0.5 μL, Taitool, Shanghai, China) was microinjected into the PrL (anteroposterior 3.0 mm, mediolateral 0.7 mm, and dorsoventral 3.3 mm) or BLA (anteroposterior -2.1 mm, mediolateral 5.0 mm, dorsoventral 8.6 mm). Following viral injection, needles were kept at the injection site for 10 min to allow for viral diffusion. Three to four weeks were allowed for viral expression. For PrL- and BLA-NAc core chemogenetic inhibition, clozapine N-oxide (2 mg/kg) was administered by intraperitoneal injection 5 min before exposure to restraint stress.

Behavioral tests. Animals were randomly grouped by different treatments. All behavioral experiments and data analysis were performed blind to the conditions of the experiments. All training/tests started at the same time (10:00 a.m.) each day, and each rat was only tested once in the following tests.

Acute restraint stress For the exposure to acute restraint stress, male rats were restrained in a cylindrical tube for 30 min or 1 h before anxiety- and obsessive-compulsive-like behavioral tests. The tube is made of clear Plexiglas, measuring 21 cm long, 6.5 cm internal diameter, with sliding plugs to allow fitting of the tube length for each animal size. The end of the tube had holes allowing free air circulation.

Elevated plus maze The elevated plus maze is a widely used test for assessing anxiety-like behavior. The apparatus consists of two open arms (50 cm × 12 cm) and two closed arms (50 cm × 12 cm with walls 40 cm in height) that are intersected at a central square (15 cm × 15 cm), with a height of 50 cm from the ground. The animals were allowed for

free exploration, and their behaviors were recorded in a 5 minute test period. The time spent on the open arms and the percentage of open arms entries were recorded and analyzed as anxiety measures using Clever TopScan (Clever Sys, Reston, VA).

Light/dark box test The light/dark box test apparatus consists of two boxes, a light one (30 cm × 30 cm × 30 cm) and a black one (30 cm × 30 cm × 30 cm). Access between the light and black box was provided by an 8 cm × 8 cm passageway. The animal was placed into the middle of the light box facing the black box. The total time spent in the light compartment in a 5 minute test period was measured using Clever TopScan (Clever Sys) and recorded as anxiety-related behavior.

Open field test Spontaneous locomotor activity was monitored by a video camera in the open field arena (50 cm × 50 cm × 50 cm). Clever TopScan (Clever Sys) quantified total distance traveled and time spent of rats in the center area during 5 minutes.

Marble burying The behavioral field was a rat cage (48.5 × 35 × 20 cm) containing 5 cm thick saw dust bedding, with 20 glass marbles (15 mm in diameter, plain dark glass) distributed in a 5 × 4 grid across the whole cage (11). Rats were placed in the cage and habituate for 10 minutes in dim light. During the testing phase, each rat was placed in the behavioral field and allowed to explore it for 30 minutes in dim light. At the end of the test, rats were removed from the cage and the number of marbles buried with bedding up to 2/3 of their depth was counted. The entire test session was also recorded on video for later analysis offline. These recordings were also scored for grooming and digging behaviors.

Patch clamp recordings in brain slices. Coronal brain slice containing the NAc core was prepared from rats of either sex and whole-cell patch clamp recordings were performed as previously described (2, 6, 7). Briefly, borosilicate glass recording electrodes were filled with either an Cs^+-methanesulfonate-based internal solution (composition in mM: 120 cesium methanesulfonate, 20 CsCl, 10 HEPES, 0.2 EGTA, 10 sodium phosphocreatine, 5 QX3144 Na_2-ATP, 0.4 Na-GTP, adjust to pH 7.2 with CsOH) or high Cl^- internal solution (composition in mM: 135 CsCl, 2 NaCl, 1 $MgSO_4$, 0.2 $CaCl_2$, 0.2 EGTA, 5 QX314, 4 Na_2-ATP, 0.4 Na-GTP, adjust to pH 7.2 with CsOH) when the effect of histamine or RAMH on miniature or evoked postsynaptic currents was recorded. The K^+-methylsulfate-based internal solution (composition in mM: 140 mM K-methylsulfate, 7 mM KCl, 2 mM $MgCl_2$, 10 mM HEPES, 0.1 mM EGTA, 4 mM Na_2-ATP, 0.4 mM GTP-Tris, adjusted to pH 7.2 with KOH) was used when the effect of histamine, 2-pyridylethylamine (2-PyEA, selective agonist for H1 receptor, 100 μM; Sigma-Aldrich), dimaprit (selective agonist for H2 receptor, 100 μM; Sigma-Aldrich) and 4-methylhistamine (selective agonist for H4 receptor, 100 μM; Tocris Bioscience) on whole cell currents were examined. Biocytin (0.05%, Sigma) was also included in the internal solution for morphological observation of the recorded medium spiny neurons combined with Alexa Fluor 488- or Alexa Fluor 594-conjugated streptavidin (1:2000, Thermo Fisher Scientific) after recordings. Electrode resistance in the bath solution was 5 to 7 MΩ and series resistance (< 25 MΩ) was monitored continuously and stable to within 20%. Medium spiny neurons, the principle/projection neurons in the NAc core, were visualized under a SliceScope two-photon microscope (MP-1000, Scientifica Ltd., Uckfield, UK). Whole cell recordings

were performed by using an Axopatch 200B amplifier (Axon Instruments, Foster City, CA) and the signals were fed into the computer through a Digidata-1550 interface (Axon Instruments) for data acquisition and analysis (pClamp 10.4, Axon Instruments).

The miniature excitatory postsynaptic currents (mEPSCs) were recorded in the presence of the tetrodetoxin (TTX, 0.3 μM; Alomone Laboratory, Jerusalem, Israel) and SR95531 (20 μM; Tocris Bioscience), which is used to block $GABA_A$ receptor-mediated inhibitory postsynaptic currents (IPSCs). For recording evoked excitatory/inhibitory postsynaptic currents (eEPSCs/eIPSCs), a concentric bipolar stimulating electrode (FHC, Bowdoinham, ME) was placed about 100 μm rostral to the recording electrode and at the same depth of the recorded neuron. eEPSCs/eIPSCs were evoked by an ISO-flex stimulus isolation unit (A.M.P.I., Jerusalem, Israel). The AMPA receptor-mediated eEPSCs were recorded when the holding potential is at -70 mV in the presence of the NMDA receptor antagonist $_D$-APV (50 μM, Tocris Bioscience), while the NMDA receptor-mediated eEPSCs were recorded at +40 mV in the presence of the AMPA receptor antagonist NBQX. For examining presynaptic mechanisms, paired stimuli (50 ms interval) were delivered every 20 s, and the paired pulse ratio was calculated as $EPSC_2/EPSC_1$. mIPSCs and eIPSCs were recorded at the holding potential of -65mV using high Cl^- pipette solution in the presence of $_D$-APV (50 μM) and NBQX (20 μM; Tocris Bioscience), with or without TTX (0.3 μM), respectively. For optogenetic stimulation (12), 470 nm light pulses were applied with a CoolLED system (pE-300white, CoolLED, Andover, UK) attached to the upright microscope. The photostimulation protocol was 10 ms pulses, 3 pulses in 3 s, repeated for 60 trials every 5 s and 5 ms pulses, 1 pulse in 30 s, repeated for 10 trials for

photostimulation of the NAc core histaminergic and glutamatergic terminals, respectively. Maximal light output at 470 nm was measured at 2 mW by optical power meter (Thorlabs, Newton, NJ).

Statistical analysis. All data were analyzed with SPSS 17.0 and presented as mean ± S.E.M. The Student's t test, one-way analysis of variance (ANOVA) was employed for statistical analysis, and Newman-Keuls post hoc testing was used to further determine the differences between groups. *P* values of < 0.05 were considered to be significant.

Supplementary Figures

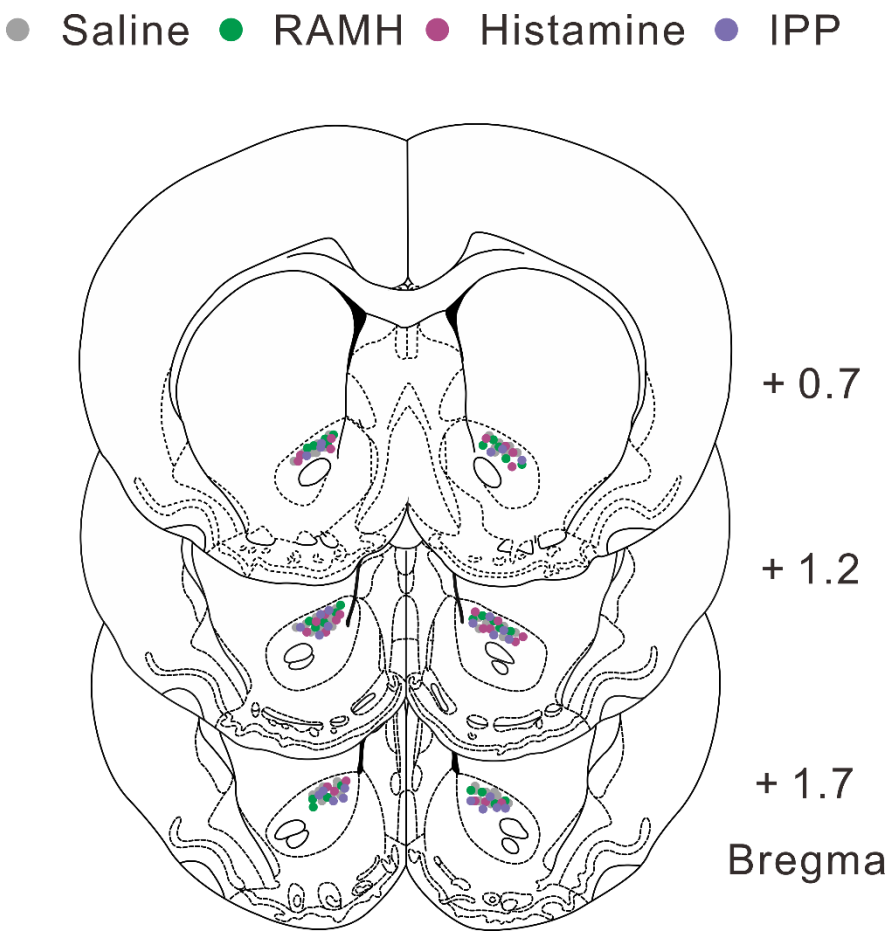

Fig. S1. Histological reconstructions showing the microinjection sites in NAc core.

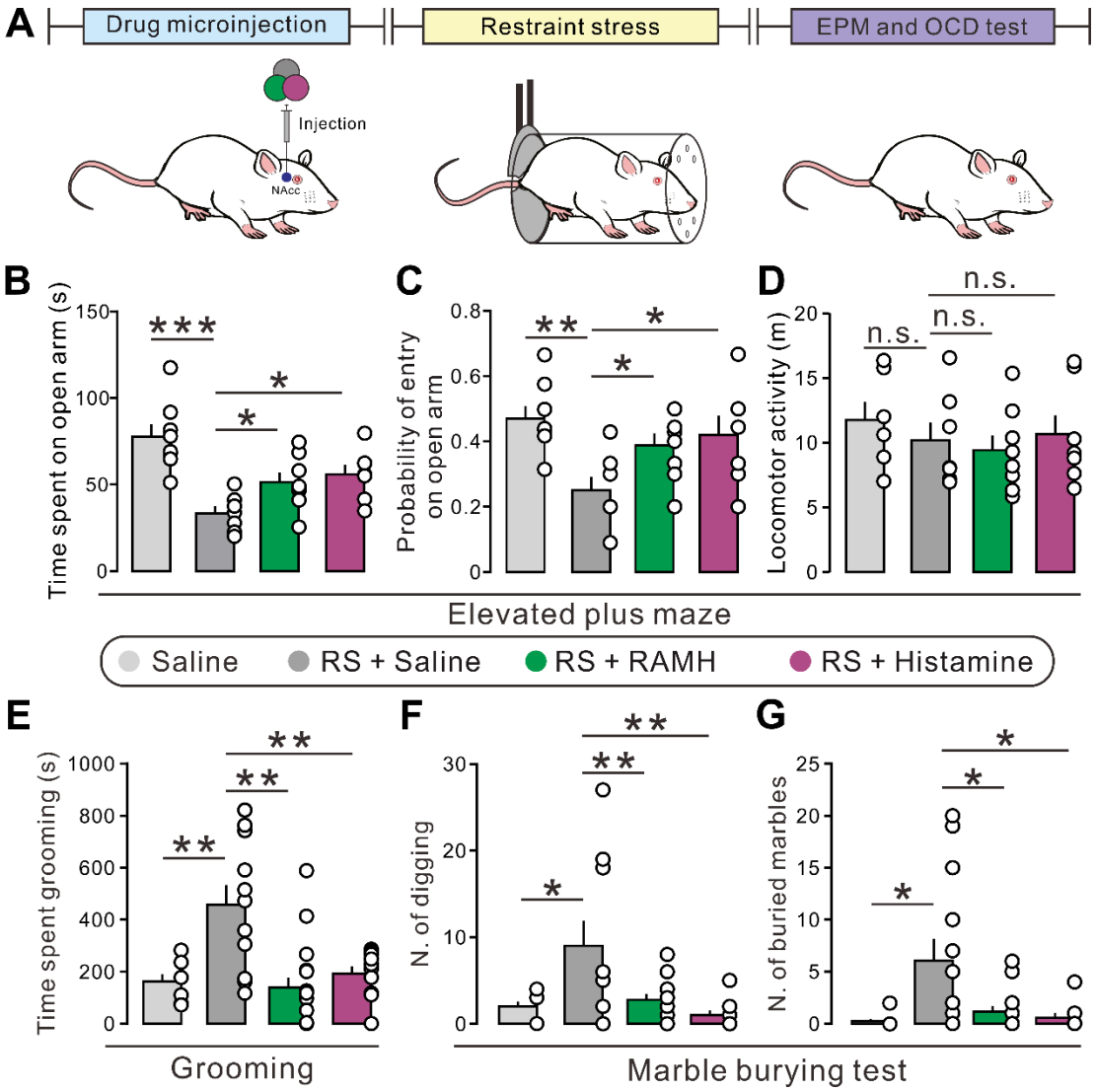

Fig. S2. Histamine improves the anxiogenic and obsessive-compulsive-like behaviors induced by restraint stress. **(A)** Scheme of experimental paradigm showing the restraint stress-induced anxiety and obsessive-compulsive-like behaviors. **(B-D)** The time spent on open arm, probability of entry into open arms and locomotor activity of normal rats with bilateral microinjection of saline (n = 8), as well as stressed rats with bilateral microinjection of saline (n = 7), RAMH (n = 8) and histamine (n = 7), in the elevated plus maze test. **(E-G)** The time spent grooming, the number of digging bouts and buried marbles

of normal rats with bilateral microinjection of saline (n = 8), as well as stressed rats with bilateral microinjection of saline (n = 11), RAMH (n = 13) and histamine (n = 9). Data are shown as means ± SEM; * P < 0.05, ** P < 0.01, *** P < 0.001, n.s., no statistical difference.

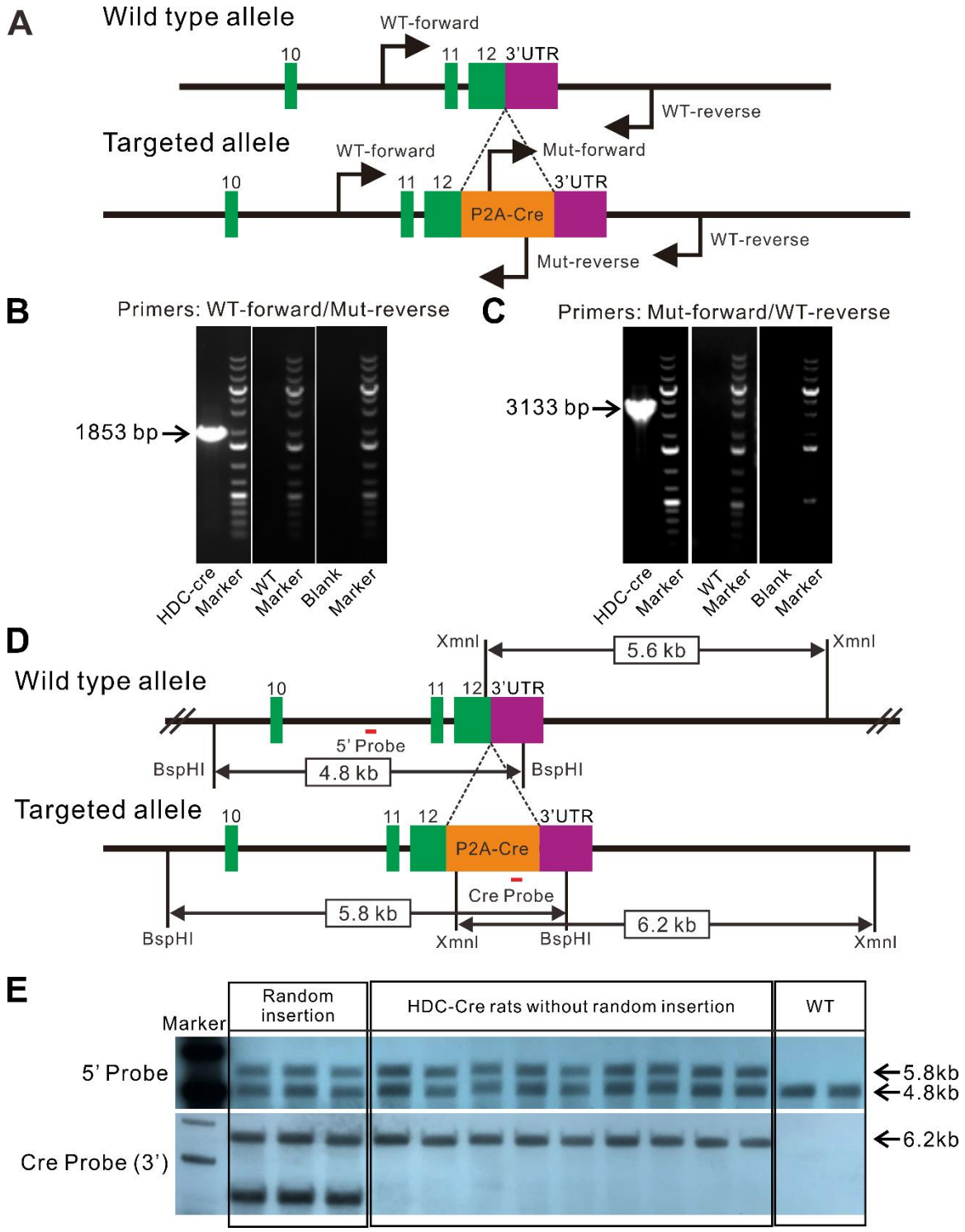

Fig. S3. Validation of the HDC-Cre transgenic rat line. **(A-C)** PCR for genotyping. (A) The PCR primer design. Both the 1853 bp (B) and the 3313 bp (C) Cre-specific PCR

products were detected in HDC-Cre transgenic rats, while were absent in WT or blank control (water). **(D, E)** Southern blot screen for correct recombination of the target locus. (D) Southern blot strategy. (E) Validation by Southern blot using two probes (5' Probe and Cre Probe (3')) and two restriction enzymes (BspHI and Xmnl). The rats with random insertion were excluded.

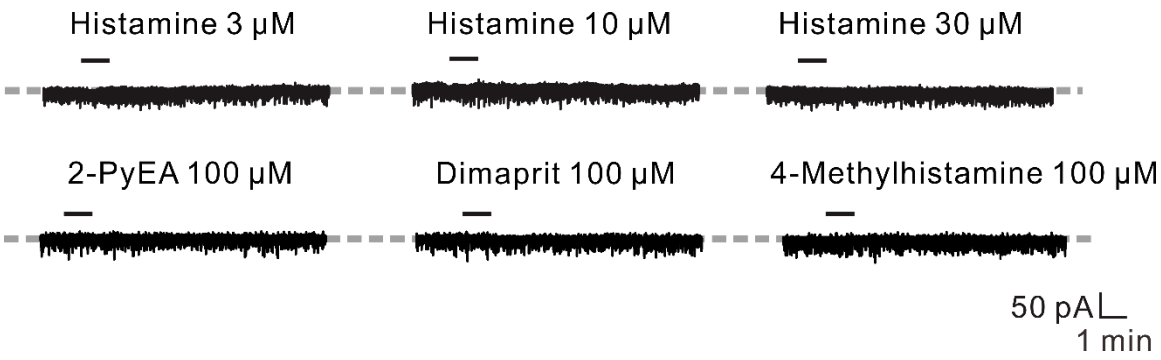

Fig. S4. Histamine (3 to 30 μM), 2-PyEA (100 μM), dimaprit (100 μM) and 4-methylhistamine (100 μM) do not induce postsynaptic inward or outward current on NAc core neurons.

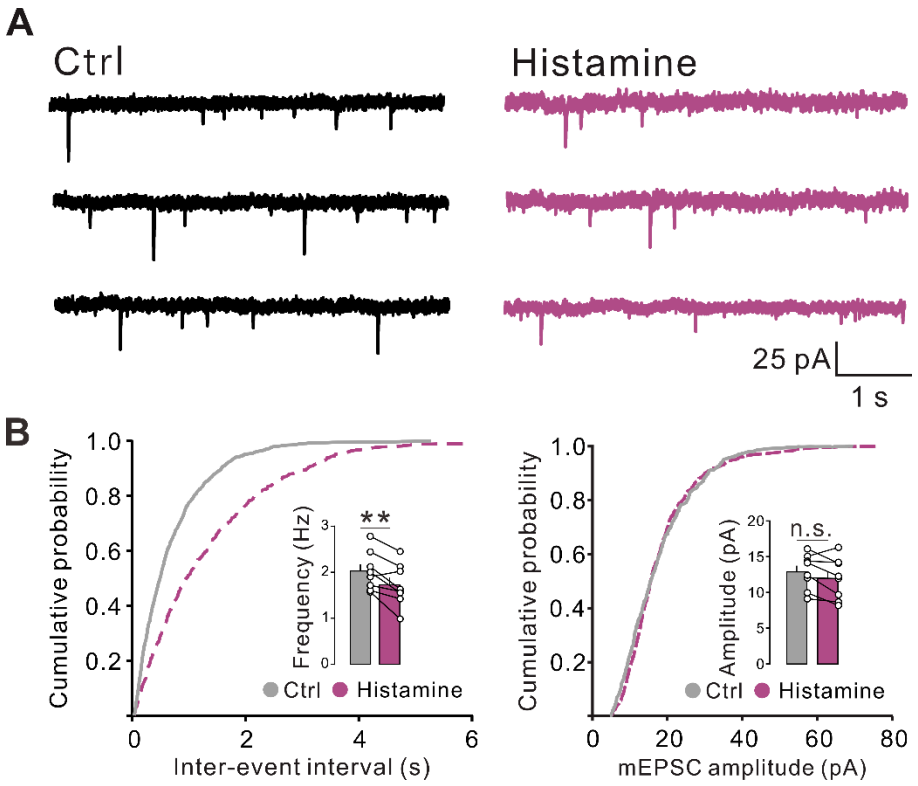

Fig. S5. Histamine inhibits the glutamatergic transmission in the NAc core neurons. **(A)** Raw current traces showing mEPSCs recorded in a NAc core neuron before and during the application of histamine (3 μM) in the presence of TTX, D-APV and SR95531. **(B)** Interevent interval and amplitude distributions for the mEPSCs in the neurons presented in (A). The inset bar graphs show histamine (n = 8) decreases the mEPSC frequency rather than amplitude in NAc core neurons. Data are shown as means ± SEM; ** $P < 0.01$, n.s., no statistical difference.

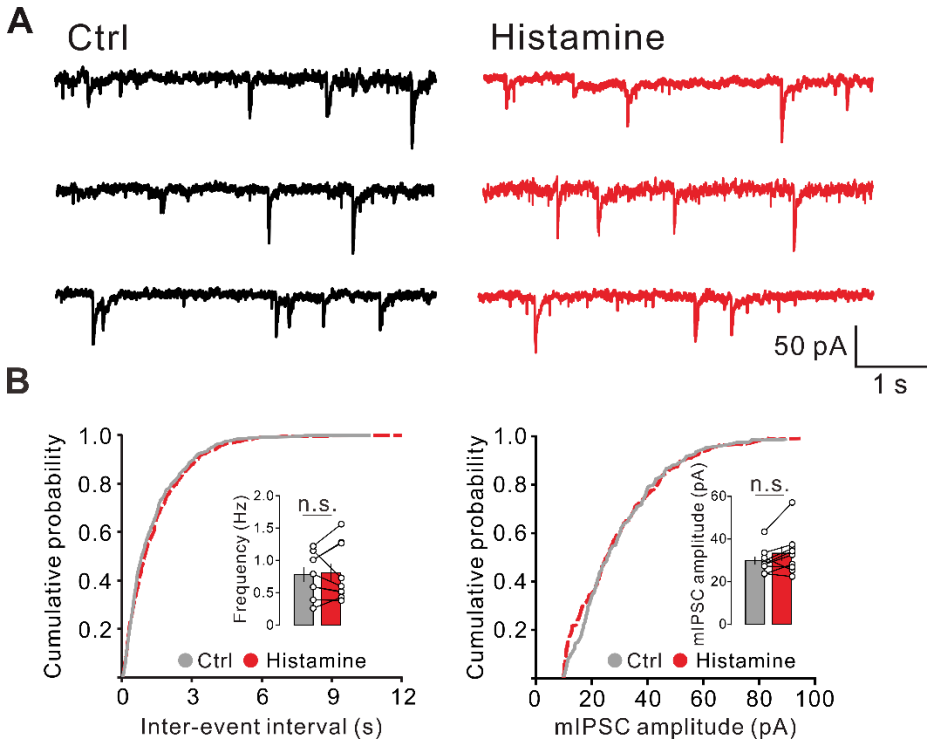

Fig. S6. Histamine does not affect GABAergic synaptic transmission in the NAc core. **(A)** Raw current traces showing mIPSCs recorded in a NAc core neuron before and during the application of histamine (3 μM) in the presence of TTX, NBQX and D-APV. **(B)** Interevent interval and amplitude distributions for the mIPSCs in the neurons presented in (A). The inset bar graphs show histamine (n = 9) does not influence the mIPSC frequency and amplitude in NAc core neurons. Data are shown as means ± SEM; n.s., no statistical difference.

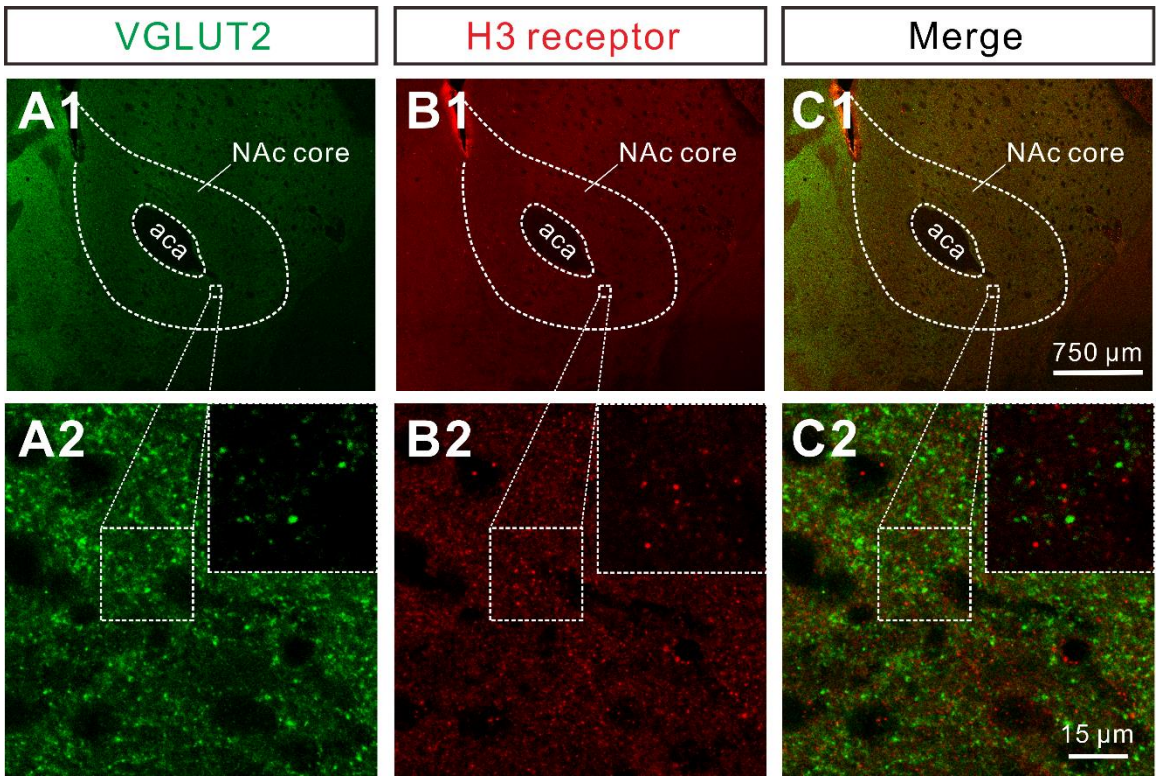

Fig. S7. H3 receptor and VGLUT2 are not colocalized in the NAc core. Double immunofluorescent labeling of VGLUT2 (*green*) (A1 and A2) and H3 receptor (*red*) (B1 and B2) in the NAc core.

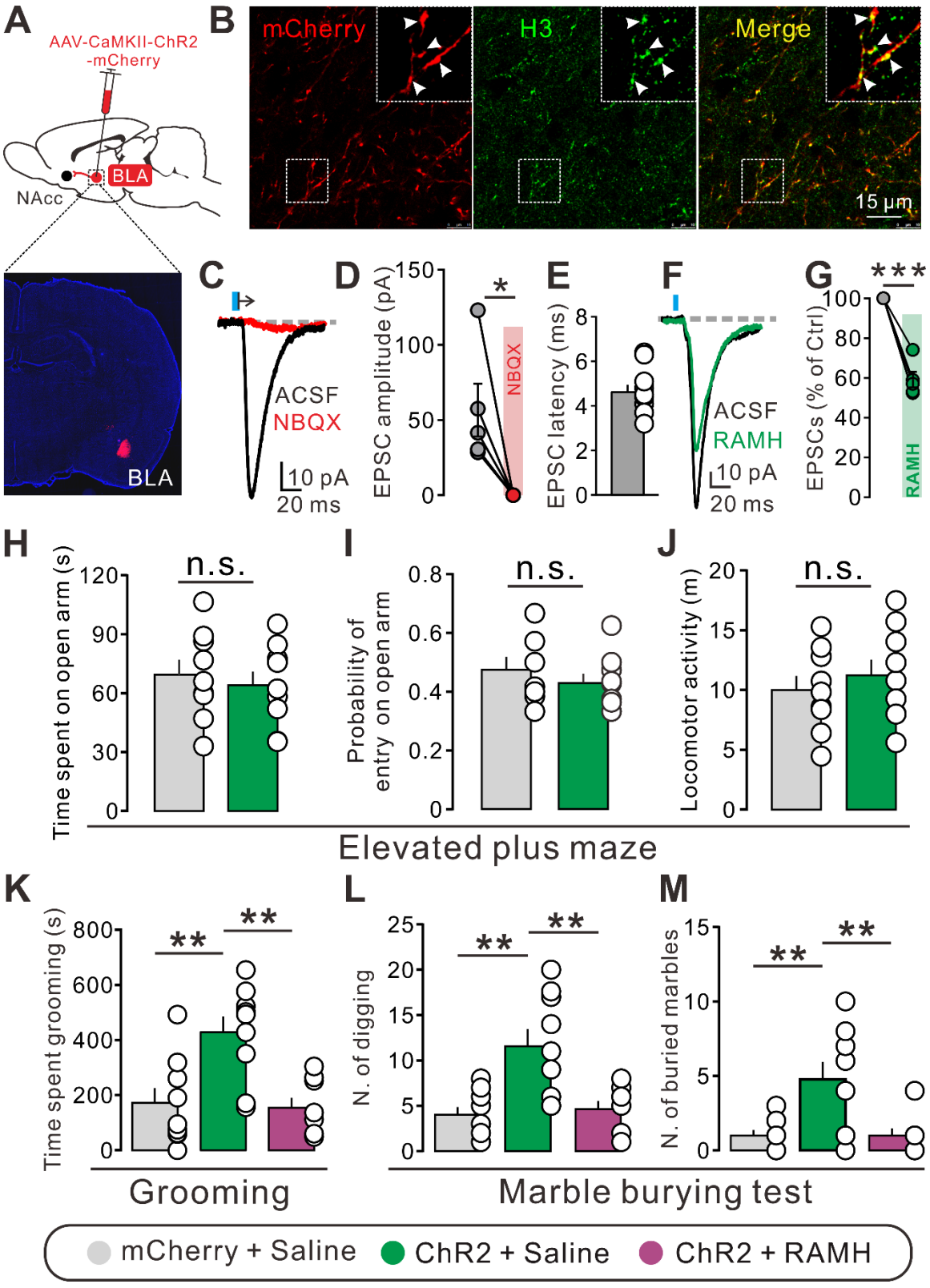
A
AAV-CaMKII-ChR2
-mCherry
BLA
NAcc
BLA
B
mCherry
H3
Merge
15 μm
C
ACSF
NBQX
10 pA
20 ms
D
EPSC amplitude (pA)
150
100
50
0
*
NBQX
E
EPSC latency (ms)
8
6
4
2
0
F
ACSF
RAMH
10 pA
20 ms
G
***
EPSCs (% of Ctrl)
100
80
60
40
20
0
RAMH
H
Time spent on open arm (s)
120
90
60
30
0
n.s.
I
Probability of
entry on open arm
0.8
0.6
0.4
0.2
0
n.s.
J
Locomotor activity (m)
20
15
10
5
0
n.s.
Elevated plus maze
K
Time spent grooming (s)
800
600
400
200
0
**
**
Grooming
L
N. of digging
25
20
15
10
5
0
**
**
M
N. of buried marbles
15
10
5
0
**
**
Marble burying test
mCherry + Saline
ChR2 + Saline
ChR2 + RAMH

Fig. S8. The effect of optogenetic activation of BLA-NAc core glutamatergic pathway on anxiogenic and obsessive-compulsive-like behaviors. **(A)** Schematics of the optogenetic manipulation of the BLA-NAc core glutamatergic pathway and confocal image of ChR2-mcherry expression in the BLA. (**B**) ChR2-mCherry (*red*) and H3 receptor (*green*) expression in the NAc core. **(C, D)** Bath application of NBQX totally blocked the light-evoked EPSCs (n = 5). **(E)** The latency between light and EPSC onset of the NAc core neurons recorded (n = 10). **(F, G)** Bath application of RAMH (3 μM) decreased the amplitude of light-evoked EPSCs (n = 5). **(H-J)** The time and probability of entry on open arm and locomotor activity of mCherry rats with bilateral microinjection of saline (n = 9), as well as ChR2 rats with bilateral microinjection of saline (n = 9). **(K-M)** The time spent grooming, and the number of digging bouts and buried marbles of mCherry rats with bilateral microinjection of saline (n = 9), as well as ChR2 rats with bilateral microinjection of saline (n = 9) and RAMH (n = 8). Data are shown as means ± SEM; * $P < 0.05$, ** $P < 0.01$, *** $P < 0.001$, n.s., no statistical difference.

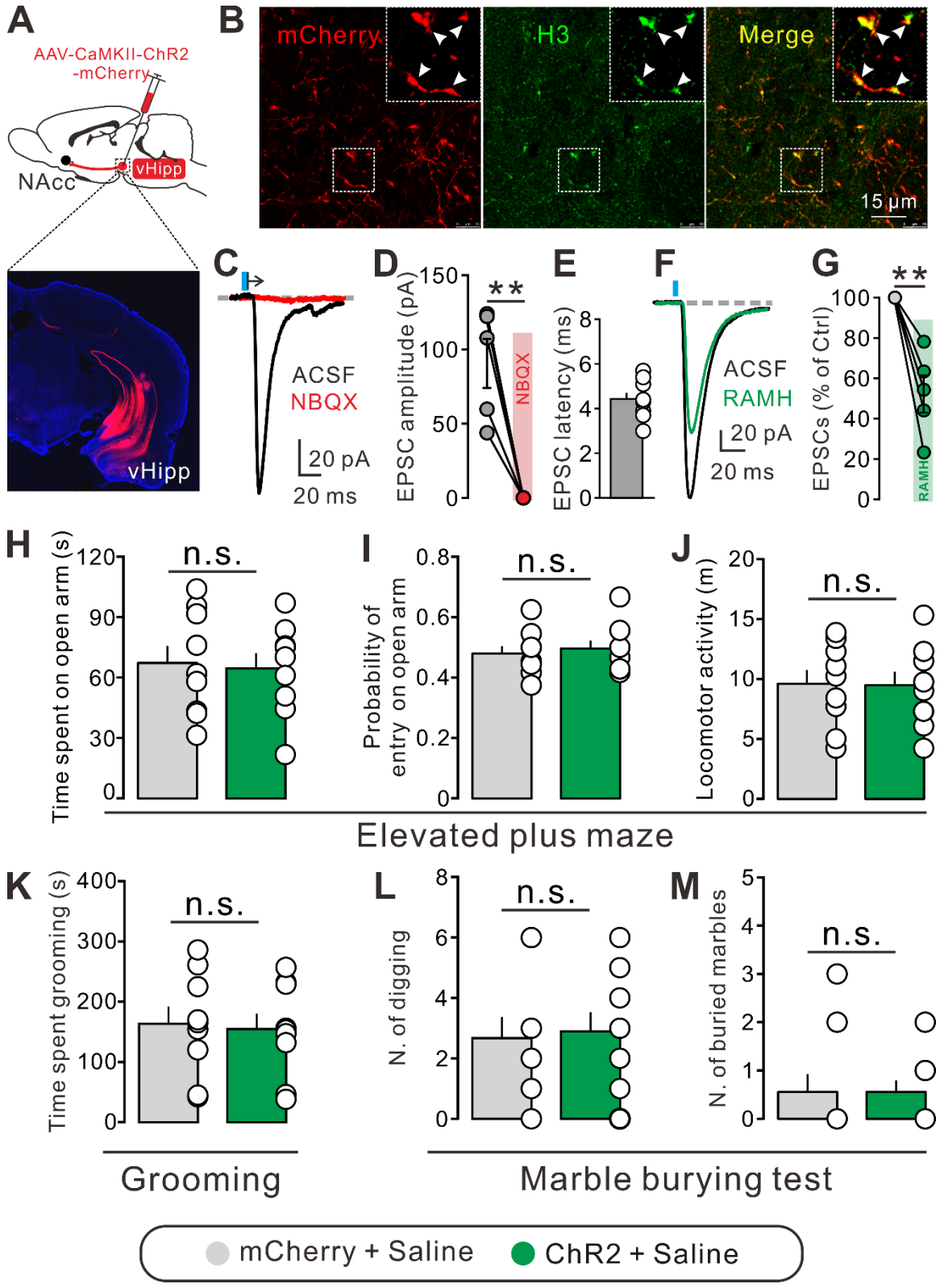
A
AAV-CaMKII-ChR2
-mCherry
NAcc
vHipp
vHipp
B
mCherry
H3
Merge
15 μm
C
ACSF
NBQX
20 pA
20 ms
D
EPSC amplitude (pA)
150
100
50
0
**
NBQX
E
EPSC latency (ms)
8
6
4
2
0
F
ACSF
RAMH
20 pA
20 ms
G
EPSCs (% of Ctrl)
100
80
60
40
20
0
**
RAMH
H
Time spent on open arm (s)
120
90
60
30
0
n.s.
I
Probability of entry on open arm
0.8
0.6
0.4
0.2
0
n.s.
J
Locomotor activity (m)
20
15
10
5
0
n.s.
Elevated plus maze
K
Time spent grooming (s)
400
300
200
100
0
n.s.
L
N. of digging
8
6
4
2
0
n.s.
M
N. of buried marbles
5
4
3
2
1
0
n.s.
Grooming
Marble burying test
mCherry + Saline
ChR2 + Saline

Fig. S9. The effect of optogenetic activation of vHipp-NAc core glutamatergic pathway on anxiogenic and obsessive-compulsive-like behaviors. **(A)** Schematics of the optogenetic manipulation of the vHipp-NAc core glutamatergic pathway and confocal image of ChR2-mcherry expression in the vHipp. (**B**) ChR2-mCherry (*red*) and H3 receptor (*green*) expression in the NAc core. **(C, D)** Bath application of NBQX totally blocked the light-evoked EPSCs (n = 5). **(E)** The latency between light and EPSC onset of the NAc core neurons recorded (n = 10). **(F, G)** Bath application of RAMH (3 μM) decreased the amplitude of light-evoked EPSCs (n = 5). **(H-J)** The time spent on open arm, probability of entry into open arms and locomotor activity of mCherry rats with bilateral microinjection of saline (n = 9), as well as ChR2 rats with bilateral microinjection of saline (n = 9). **(K-M)** The time spent grooming, and the number of digging bouts and buried marbles of mCherry rats with bilateral microinjection of saline (n = 9), as well as ChR2 rats with bilateral microinjection of saline (n = 9). Data are shown as means ± SEM; ** P < 0.01, n.s., no statistical difference.

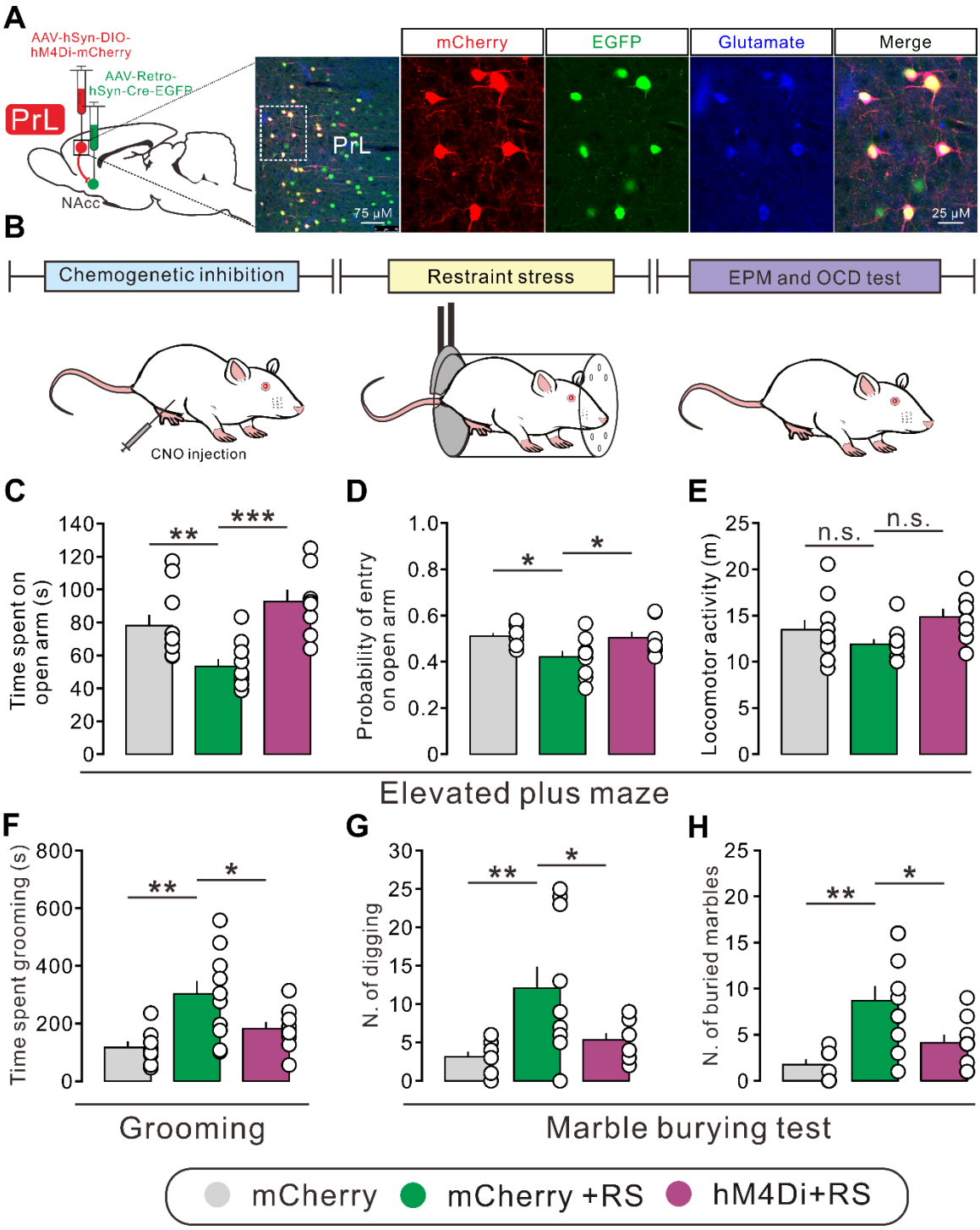
A
AAV-hSyn-DIO-hM4Di-mCherry
AAV-Retro-hSyn-Cre-EGFP
PrL
NAcc
PrL
75 μM
mCherry
EGFP
Glutamate
Merge
25 μM
B
Chemogenetic inhibition
Restraint stress
EPM and OCD test
CNO injection
C
Time spent on open arm (s)
D
Probability of entry on open arm
E
Locomotor activity (m)
n.s.
n.s.
Elevated plus maze
F
Time spent grooming (s)
Grooming
G
N. of digging
H
N. of buried marbles
Marble burying test
mCherry
mCherry +RS
hM4Di+RS

Fig. S10. The effect of chemogenetic inhibition of the PrL-NAc core glutamatergic pathway on the anxiogenic and obsessive-compulsive-like behaviors induced by restraint stress. (**A**) Schematics of the chemogenetic inhibition of the PrL-NAc core pathway and confocal image of hM4Di-mcherry expression (*red*) on retrogradely labeled (*green*) glutamatergic neurons (*blue*) in the PrL projecting to the NAc core. (**B**) Scheme of experimental paradigm showing the restraint stress-induced anxiety and obsessive-compulsive-like behaviors in rats that underwent chemogenetic inhibition. (**C**-**E**) The time spent on open arm, probability of entry into open arms and locomotor activity of control (n = 10) or stressed (n = 10) mCherry rats with intraperitoneal administration of clozapine N-oxide (CNO), as well as stressed hM4Di rats (n = 8) with intraperitoneal administration of CNO. (**F**-**H**) The time spent grooming, the number of digging bouts and buried marbles of control (n = 8) or stressed (n = 10) mCherry rats with intraperitoneal administration of CNO, as well as stressed hM4Di rats (n = 9) with intraperitoneal administration of CNO. Data are shown as means ± SEM; * $P < 0.05$, ** $P < 0.01$, *** $P < 0.001$, n.s., no statistical difference.

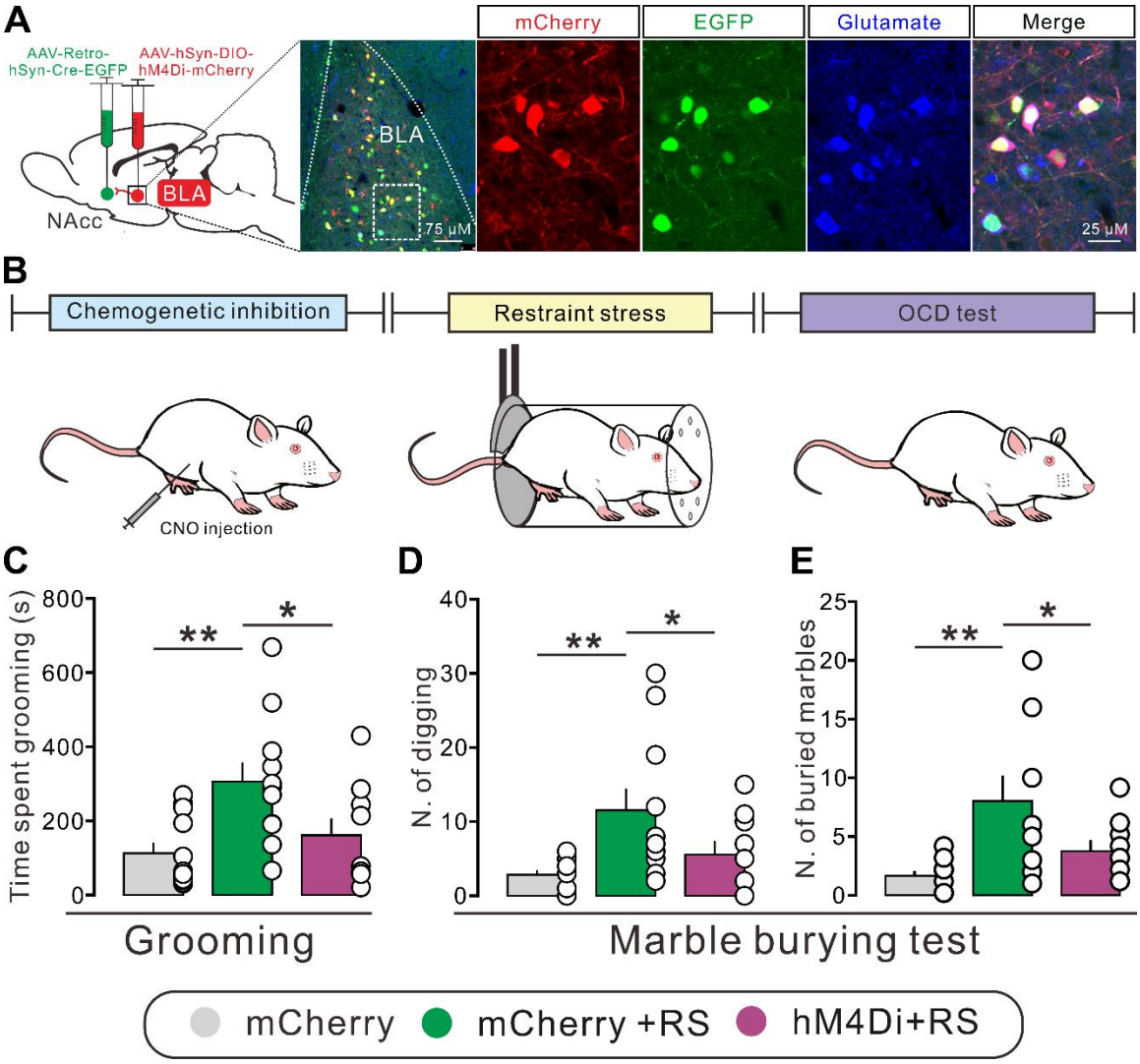

Fig. S11. The effect of chemogenetic inhibition of the BLA-NAc core glutamatergic pathway on the obsessive-compulsive-like behaviors induced by restraint stress. (**A**) Schematics of the chemogenetic inhibition of the BLA-NAc core pathway and confocal image of hM4Di-mcherry expression (*red*) on retrogradely labeled (*green*) glutamatergic neurons (*blue*) in the BLA projecting to the NAc core. (**B**) Scheme of experimental paradigm showing the obsessive-compulsive-like behaviors in rats that underwent chemogenetic inhibition. (**C-E**) The time spent grooming, the number of digging bouts and

buried marbles of control (n = 12) or stressed (n = 11) mCherry rats with intraperitoneal administration of clozapine N-oxide (CNO), as well as stressed hM4Di rats (n = 9) with intraperitoneal administration of CNO. Data are shown as means ± SEM; * $P < 0.05$, ** $P < 0.01$.

Supplementary Table

Table S1. Statistical report for each experiment.

Figure panel	Test used	Statistical result
Figure 1H	Unpaired t test	t(8) = 3.064, P = 0.016
Figure 1I	One-way ANOVA	F(3, 36) = 11.700, P < 0.001
	Newman-Keuls post hoc test	P = 0.010, 0.015, and 0.043
Figure 1J	One-way ANOVA	F(3, 36) = 10.500, P < 0.001
	Newman-Keuls post hoc test	P = 0.015, 0.027, and 0.047
Figure 1K	One-way ANOVA	F(3, 36) = 11.160, P < 0.001
	Newman-Keuls post hoc test	P = 0.013, 0.037, and 0.030.
Figure 1L	One-way ANOVA	F(3, 36) = 11.720, P < 0.001
	Newman-Keuls post hoc test	P = 0.019, 0.011, and 0.032
Figure 1M	One-way ANOVA	F(3, 36) = 1.836, P = 0.158
	Newman-Keuls post hoc test	P = 0.572, 0.398, and 0.291
Figure 2E	Unpaired t test (mCherry + Saline *vs.* RS + mCherry + Saline)	t(12) = 2.202, P = 0.048
	One-way ANOVA	F(2, 20) = 7.491, P = 0.004
	Newman-Keuls post hoc test	P = 0.011 and 0.004
Figure 2F	Unpaired t test (mCherry + Saline *vs.* RS + mCherry + Saline)	t(12) = 3.253, P = 0.007
	One-way ANOVA	F(2, 20) = 4.285, P = 0.028
	Newman-Keuls post hoc test	P = 0.032 and 0.039
Figure 2G	Unpaired t test (mCherry + Saline *vs.* RS + mCherry + Saline)	t(12) = 0.041, P = 0.968
	One-way ANOVA	F(2, 20) = 0.185, P = 0.833
	Newman-Keuls post hoc test	P = 0.817 and 0.761
Figure 2H	Unpaired t test (mCherry + Saline *vs.* RS + mCherry + Saline)	t(14) = 2.218, P = 0.044
	One-way ANOVA	F(2, 23) = 4.746, P = 0.019
	Newman-Keuls post hoc test	P = 0.034 and 0.015
Figure 2I	Unpaired t test (mCherry + Saline *vs.* RS + mCherry + Saline)	t(14) = 4.288, P < 0.001
	One-way ANOVA	F(2, 23) = 4.150, P = 0.029
	Newman-Keuls post hoc test	P = 0.046 and 0.030
Figure 2J	Unpaired t test (mCherry + Saline *vs.* RS + mCherry + Saline)	t(14) = 3.309, P = 0.005
	One-way ANOVA	F(2, 23) = 4.527, P = 0.022
	Newman-Keuls post hoc test	P = 0.025 and 0.029
Figure 3B (Left)	Paired t test	t(6) = 3.969, P = 0.007
Figure 3B (Right)	Paired t test	t(6) = 0.610, P = 0.564
Figure 3D (Left)	Paired t test	t(6) = 0.455, P = 0.665

Figure panel	Test used	Statistical result
Figure 3D (Right)	Paired t test	t(6) = 1.561, P = 0.170
Figure 3F	Paired t test	t(28) = 18.900, P < 0.001
Figure 3G	Paired t test	t(11) = 13.980, P < 0.001
Figure 4A	Paired t test	t(20) = 19.34, P < 0.001
Figure 4B	Paired t test	t(7) = 9.65, P < 0.001
Figure 4C	Paired t test	t(8) = 0.746, P = 0.477
Figure 4D	Paired t test	t(9) = 9.936, P < 0.001
Figure 4E	Paired t test	t(7) = 1.312, P = 0.231
Figure 4F	Paired t test (Histamine *vs.* Control)	t(6) = 14.490, P < 0.001
	Paired t test (Histamine + IPP *vs.* IPP)	t(6) = 2.191, P = 0.071
Figure 4I	Paired t test (Light on *vs.* control)	t(7) = 7.310, P < 0.001
	Paired t test (Light on + IPP *vs.* IPP)	t(5) = 0.524, P = 0.623
Figure 5D	Paired t test	t(4) = 4.166, P = 0.014
Figure 5G	Paired t test	t(4) = 6.382, P = 0.003
Figure 5I	One-way ANOVA	F(3, 34) = 5.814, P = 0.003
	Newman-Keuls post hoc test	P = 0.002, 0.015, and 0.029
Figure 5J	One-way ANOVA	F(3, 34) = 4.981, P = 0.006
	Newman-Keuls post hoc test	P = 0.011, 0.007 and 0.017
Figure 5K	One-way ANOVA	F(3, 34) = 0.891, P = 0.456
	Newman-Keuls post hoc test	P = 0.876, 0.928 and 0.280
Figure 5L	One-way ANOVA	F(3, 19) = 4.715, P = 0.013
	Newman-Keuls post hoc test	P = 0.009, 0.028 and 0.026
Figure 5M	One-way ANOVA	F(3, 19) = 8.737, P = 0.001
	Newman-Keuls post hoc test	P = 0.001, 0.002 and 0.011
Figure 5N	One-way ANOVA	F(3, 19) = 6.293, P = 0.004
	Newman-Keuls post hoc test	P = 0.006, 0.009 and 0.010
Figure S2B	One-way ANOVA	F(3, 26) = 9.985, P < 0.001
	Newman-Keuls post hoc test	P < 0.001, = 0.037 and 0.034
Figure S2C	One-way ANOVA	F(3, 26) = 4.510, P = 0.011
	Newman-Keuls post hoc test	P = 0.008, 0.036 and 0.035
Figure S2D	One-way ANOVA	F(3, 26) = 0.599, P = 0.621
	Newman-Keuls post hoc test	P = 0.663, 0.697 and 0.813
Figure S2E	One-way ANOVA	F(3, 37) = 7.080, P = 0.001
	Newman-Keuls post hoc test	P = 0.003, 0.001 and 0.003
Figure S2F	One-way ANOVA	F(3, 37) = 4.939, P = 0.006
	Newman-Keuls post hoc test	P = 0.019, 0.005 and 0.009
Figure S2G	One-way ANOVA	F(3, 37) = 3.871, P = 0.017
	Newman-Keuls post hoc test	P = 0.040, 0.011 and 0.025
Figure S5B(Left)	Paired t test	t(7) = 3.702, P = 0.008
Figure S5B (Right)	Paired t test	t(7) = 2.098, P = 0.074
Figure S6B(Left)	Paired t test	t(8) = 0.355, P = 0.732
Figure S6B (Right)	Paired t test	t(8) = 1.849, P = 0.102

Figure panel	Test used	Statistical result
Figure S8D	Paired t test	t(4) = 3.217, P = 0.032
Figure S8G	Paired t test	t(4) = 10.370, P < 0.001
Figure S8H	Unpaired t test	t(16) = 0.511, P = 0.616
Figure S8I	Unpaired t test	t(16) = 0.831, P = 0.418
Figure S8J	Unpaired t test	t(16) = 0.702, P = 0.493
Figure S8K	One-way ANOVA	F(2, 23) = 9.195, P = 0.001
	Newman-Keuls post hoc test	P = 0.002 and 0.003
Figure S8L	One-way ANOVA	F(2, 23) = 9.907, P = 0.001
	Newman-Keuls post hoc test	P = 0.002 and 0.002
Figure S8M	One-way ANOVA	F(2, 23) = 8.078, P = 0.002
	Newman-Keuls post hoc test	P = 0.002 and 0.007
Figure S9D	Paired t test	t(4) = 5.501, P = 0.005
Figure S9G	Paired t test	t(4) = 5.119, P = 0.007
Figure S9H	Unpaired t test	t(16) = 0.231, P = 0.820
Figure S9I	Unpaired t test	t(16) = 0.472, P = 0.643
Figure S9J	Unpaired t test	t(16) = 0.066, P = 0.948
Figure S9K	Unpaired t test	t(16) = 0.225, P = 0.825
Figure S9L	Unpaired t test	t(16) = 0.234, P = 0.818
Figure S9M	Unpaired t test	t(16) = 0, P > 0.999
Figure S10C	One-way ANOVA	F(2, 25) = 10.11, P = 0.001
	Newman-Keuls post hoc test	P = 0.007 and <0.001
Figure S10D	One-way ANOVA	F(2, 25) = 5.319, P = 0.012
	Newman-Keuls post hoc test	P = 0.017 and 0.017
Figure S10E	One-way ANOVA	F(2, 25) = 2.798, P = 0.080
	Newman-Keuls post hoc test	P = 0.199 and 0.067
Figure S10F	One-way ANOVA	F(2, 24) = 6.339, P = 0.006
	Newman-Keuls post hoc test	P = 0.005 and 0.032
Figure S10G	One-way ANOVA	F(2, 24) = 6.112, P = 0.007
	Newman-Keuls post hoc test	P = 0.008 and 0.017
Figure S10H	One-way ANOVA	F(2, 24) = 8.707, P = 0.001
	Newman-Keuls post hoc test	P = 0.001 and 0.011
Figure S11C	One-way ANOVA	F(2, 29) = 5.970, P = 0.007
	Newman-Keuls post hoc test	P = 0.006 and 0.027
Figure S11D	One-way ANOVA	F(2, 29) = 5.388, P = 0.010
	Newman-Keuls post hoc test	P = 0.008 and 0.048
Figure S11E	One-way ANOVA	F(2, 29) = 5.610, P = 0.009
	Newman-Keuls post hoc test	P = 0.007 and 0.045

SI References

1. National Research Council, *Guide for the Care and Use of Laboratory Animals* (National Academies Press, Washington, DC, ed. 8, 2011).
2. Y. Wang, Z. P. Chen, Q. X. Zhuang, X. Y. Zhang, H. Z. Li, J. J. Wang, J. N. Zhu, Role of Corticotropin-Releasing Factor in Cerebellar Motor Control and Ataxia. *Curr. Biol.* 10.1016/j.cub.2017.07.035 (2017).
3. Q. X. Zhuang, G. Y. Li, B. Li, C. Z. Zhang, X. Y. Zhang, K. Xi, H. Z. Li, J. J. Wang, J. N. Zhu, Regularizing firing patterns of rat subthalamic neurons ameliorates parkinsonian motor deficits. *J Clin Invest* **128**, 5413-5427 (2018).
4. M. J. Ji, X. Y. Zhang, Z. Chen, J. J. Wang, J. N. Zhu, Orexin prevents depressive-like behavior by promoting stress resilience. *Mol Psychiatry* **24**, 282-293 (2019).
5. G. Paxinos, C. Watson, The rat brain in stereotaxic coordinates, 7th edn. *Academic Press, San Diego, CA* (2014).
6. J. Zhang, B. Li, L. Yu, Y. C. He, H. Z. Li, J. N. Zhu, J. J. Wang, A role for orexin in central vestibular motor control. *Neuron* **69**, 793-804 (2011).
7. M. J. Ji, X. Y. Zhang, X. C. Peng, Y. X. Zhang, Z. Chen, L. Yu, J. J. Wang, J. N. Zhu, Histamine Excites Rat GABAergic Ventral Pallidum Neurons via Co-activation of H1 and H2 Receptors. *Neurosci Bull* **34**, 1029-1036 (2018).
8. R. H. Williams, M. J. Chee, D. Kroeger, L. L. Ferrari, E. Maratos-Flier, T. E. Scammell, E. Arrigoni, Optogenetic-mediated release of histamine reveals distal and autoregulatory mechanisms for controlling arousal. *J Neurosci* **34**, 6023-6029 (2014).
9. R. C. Bagot, E. M. Parise, C. J. Pena, H. X. Zhang, I. Maze, D. Chaudhury, B. Persaud, R. Cachope, C. A. Bolanos-Guzman, J. F. Cheer, K. Deisseroth, M. H. Han, E. J. Nestler, Ventral hippocampal afferents to the nucleus accumbens regulate susceptibility to depression. *Nat Commun* **6**, 7062 (2015).
10. C. J. Shen, D. Zheng, K. X. Li, J. M. Yang, H. Q. Pan, X. D. Yu, J. Y. Fu, Y. Zhu, Q. X. Sun, M. Y. Tang, Y. Zhang, P. Sun, Y. Xie, S. Duan, H. Hu, X. M. Li, Cannabinoid CB1 receptors in the amygdalar cholecystokinin glutamatergic afferents to nucleus accumbens modulate depressive-like behavior. *Nat Med* **25**, 337-349 (2019).
11. L. Verma, D. Agrawal, N. S. Jain, Enhanced central histaminergic transmission attenuates compulsive-like behavior in mice. *Neuropharmacology* **138**, 106-117 (2018).
12. A. K. Lahiri, M. D. Bevan, Dopaminergic Transmission Rapidly and Persistently Enhances Excitability of D1 Receptor-Expressing Striatal Projection Neurons. *Neuron* **106**, 277-290 e276 (2020).